Cell Calcium 49 (2011) 56–65

Cell Calcium

journal homepage: www.elsevier.com/locate/ceca

Inhibition of spontaneous activity of rabbit atrioventricular node cells by KB-R7943 and inhibitors of sarcoplasmic reticulum Ca^{2+} ATPase

Hongwei Cheng[a], Godfrey L. Smith[b], Jules C. Hancox[a,*], Clive H. Orchard[a,**]

[a] School of Physiology and Pharmacology, Medical Sciences Building, University of Bristol, Bristol BS8 1TD, UK
[b] Cardiovascular Physiology, University of Glasgow, Glasgow G12 8QQ, UK

ARTICLE INFO

Article history:
Received 20 August 2010
Received in revised form
11 November 2010
Accepted 17 November 2010
Available online 15 December 2010

Keywords:
Atrioventricular node (AVN)
Calcium
KB-R7943
Sarcoplasmic reticulum (SR)
Spontaneous activity
Sodium–calcium exchange (NCX)
Thapsigargin

ABSTRACT

The atrioventricular node (AVN) can act as a subsidiary cardiac pacemaker if the sinoatrial node fails. In this study, we investigated the effects of the Na–Ca exchange (NCX) inhibitor KB-R7943, and inhibition of the sarcoplasmic reticulum calcium ATPase (SERCA), using thapsigargin or cyclopiazonic acid (CPA), on spontaneous action potentials (APs) and $[Ca^{2+}]_i$ transients from cells isolated from the rabbit AVN. Spontaneous $[Ca^{2+}]_i$ transients were monitored from undialysed AVN cells at 37 °C using Fluo-4. In separate experiments, spontaneous APs and ionic currents were recorded using the whole-cell patch clamp technique. Rapid application of 5 μM KB-R7943 slowed or stopped spontaneous APs and $[Ca^{2+}]_i$ transients. However, in voltage clamp experiments in addition to blocking NCX current (I_{NCX}) KB-R7943 partially inhibited L-type calcium current ($I_{Ca,L}$). Rapid reduction of external $[Na^+]$ also abolished spontaneous activity. Inhibition of SERCA (using 2.5 μM thapsigargin or 30 μM CPA) also slowed or stopped spontaneous APs and $[Ca^{2+}]_i$ transients. Our findings are consistent with the hypothesis that sarcoplasmic reticulum (SR) Ca^{2+} release influences spontaneous activity in AVN cells, and that this occurs via $[Ca^{2+}]_i$-activated I_{NCX}; however, the inhibitory action of KB-R7943 on $I_{Ca,L}$ means that care is required in the interpretation of data obtained using this compound.

1. Introduction

The cardiac atrioventricular node (AVN) conducts electrical excitation from the atria to the ventricles. Its slow rate of conduction co-ordinates atrial and ventricular contraction and can protect against some types of arrhythmia [1,2]. The AVN also possesses intrinsic pacemaker activity, although the mechanisms underlying this activity are not fully understood. It has been suggested that in the sinoatrial node (SAN) spontaneous Ca^{2+} release from the sarcoplasmic reticulum (SR) contributes to pacemaking: early work showed that inhibition of SR Ca^{2+} release decreases the spontaneous frequency of the SAN [3–5], and more recent work has provided evidence that sodium–calcium exchange (NCX) activity is necessary for SAN pacemaker activity (e.g. [6–8]), with Ca^{2+} release from the SR contributing to pacemaking by activating inward NCX current (I_{NCX}) [3–10].

Less is known about the role of Ca^{2+} in AVN pacemaking. Rabbit AVN cells exhibit $[Ca^{2+}]_i$ transients during spontaneous activity and possess functional NCX, with an I_{NCX} density similar to that in ventricular myocytes [11–13]. Recent evidence from experiments with the SR inhibitor ryanodine implicates Ca^{2+} release from the SR in pacemaking in intact AVN preparations [14], and indicates that the rate of spontaneous action potentials (APs) and $[Ca^{2+}]_i$ transients in rabbit AVN cells [13] is sensitive to SR inhibition, consistent with a link between Ca^{2+} handling and spontaneous activity in these cells.

The present study was designed to investigate further the role of Ca^{2+} in the spontaneous activity of the AVN, in particular the contribution of SR Ca^{2+} release to AVN pacemaking and whether this involves I_{NCX}. The NCX inhibitor KB-R7943, which has been used extensively in studies of atrial, ventricular and SAN cells (e.g. [8,15–18]), and the SR Ca^{2+} ATPase (SERCA) inhibitors thapsigargin [19] and cyclopiazonic acid (CPA) [20], were used to investigate the role of NCX and SR Ca^{2+} release in the generation of spontaneous APs and $[Ca^{2+}]_i$ transients in cells isolated from the rabbit AVN.

2. Methods

2.1. AVN myocyte isolation

Male New Zealand White rabbits (2–3 kg) were killed humanely in accordance with UK Home Office legislation, and AVN cells isolated from the heart using a combination of enzymatic and mechanical dispersion, as described previously [21]. In brief, hearts

* Corresponding author. Tel.: +44 117 33 12292.
** Corresponding author. Tel.: +44 117 33 11532.
E-mail addresses: jules.hancox@bristol.ac.uk (J.C. Hancox), clive.orchard@bristol.ac.uk (C.H. Orchard).

0143-4160 © 2010 Elsevier Ltd. Open access under CC BY-NC-ND license.
doi:10.1016/j.ceca.2010.11.008

were Langendorff-perfused at 37 °C with Ca^{2+}-containing solution, then Ca^{2+}-free solution containing EGTA (100 μM), and then enzyme-containing solution (1 mg/ml collagenase, type I, Worthington, USA and 0.1 mg/ml protease, type XIV, Sigma, USA), followed by removal of the AVN, identified by its relation to anatomical landmarks [22]. AVN cells were dispersed from the AVN and re-suspended and stored in refrigerated (4 °C) Kraftbruhe 'KB' solution [23] until use.

2.2. Solutions and chemicals

All chemicals were purchased from Sigma–Aldrich (UK), and all solutions were made with deionised Milli-Q water (Millipore Systems, USA), unless stated otherwise. The cell isolation and 'KB' solutions have been described previously [21,24]. The normal Tyrode solution used to superfuse cells contained (in mM) [25]: 140 NaCl, 4 KCl, 2 $CaCl_2$, 1 $MgCl_2$, 10 glucose, 5 HEPES (pH 7.4 with NaOH). For spontaneous action potential recording, the K^+-based pipette solution contained (in mM) [26]: 110 KCl, 10 NaCl, 0.4 $MgCl_2$, 10 HEPES, 5 glucose, 5 K_2ATP, 0.5 GTP-Tris (pH 7.1 with KOH). For L-type calcium current ($I_{Ca,L}$) recording, the internal solution was similar, except that KCl was replaced with CsCl, and 5 mM BAPTA was added [27]. For I_{NCX} recording, the internal solution was also Cs^+-based, and contained (in mM) [12]: 110 CsCl, 10 NaCl, 0.4 $MgCl_2$, 1 $CaCl_2$, 5 EGTA, 10 HEPES, 5 glucose, 20 TEACl (pH 7.2 with CsOH), and the external solution was potassium-free Tyrode containing 10 μM nitrendipine (to inhibit L-type calcium current) and 10 μM strophanthidin (to inhibit the Na^+/K^+ pump). The low-sodium Tyrode solution used to inhibit forward mode NCX contained 40 mM NaCl (LiCl replacement). KB-R7943 (Tocris, USA), thapsigargin and CPA were dissolved in dimethyl sulfoxide (DMSO) to produce stock solutions of 5, 2.5, and 30 mM respectively, which were kept at −20 °C. Nickel (Ni^{2+}) chloride, used to block I_{NCX}, was made up as 5 M stock solution which was kept at −4 °C.

2.3. Electrophysiological recording

AVN cells were transferred to an experimental chamber mounted on the stage of an inverted microscope (Eclipse TE2000-U, Nikon, Japan) and superfused with Tyrode solution. Whole-cell patch-clamp experiments were performed using an AxoPatch-1D amplifier (Axon Instruments, USA). Patch-pipettes (A-M Systems, USA) were pulled using a Narishige vertical electrode puller (Narishige PP-83, Japan), and heat-polished to a final resistance of 2–3 MΩ (Narishige MF-83, Japan). Protocols were generated and data recorded using pClamp 10 software (Axon Instruments, USA) via an analogue-to-digital converter (Digidata 1322; Axon Instruments/Molecular Devices, USA). Spontaneous action potentials were recorded continuously using gap-free acquisition mode by current clamping with zero-current input. APs were digitised at 2 kHz. Membrane currents were recorded in whole-cell voltage-clamp mode, and digitised at 10 kHz. I_{NCX} was measured as 5 mM Ni^{2+}-sensitive current elicited by voltage ramp commands (at a frequency of 0.33 Hz) from +60 to −80 mV over 250 ms from a holding potential of −40 mV, and $I_{Ca,L}$ was elicited using test pulses from −40 to 0 mV at 0.2 Hz.

Once the whole-cell patch-clamp recording configuration had been obtained, cell superfusion was via a rapid solution exchange (<1 s) device [28], which was used to change superfusate. All superfusates were maintained at 35–37 °C.

2.4. $[Ca^{2+}]_i$ imaging and calcium transient analysis

$[Ca^{2+}]_i$ was monitored in intact, undialysed AVN myocytes loaded with the fluorescent Ca^{2+} indicator Fluo-4. Cells were incubated with 5 μM Fluo-4 AM (Invitrogen, USA) for 5 min in KB solution at 37 °C, and then centrifuged and re-suspended in Tyrode solution for 30 min at room temperature for dye de-esterification, before being placed in the experimental chamber on the stage of a laser-scanning confocal microscope (Zeiss LSM Pascal, Germany). Transverse line scan images of spontaneously beating AVN cells were obtained through the centre of the cell, with a slice depth of ~1 μm, at 2 ms/line, during superfusion with control and test Tyrode solutions at 35–37 °C. Fluo-4 was excited with 488 nm light, and emitted fluorescence measured at >505 nm. Averaged line scan fluorescence was normalized to diastolic fluorescence to give F/F_0 [29]. $[Ca^{2+}]_i$ transient amplitude was defined as the difference between baseline and peak.

2.5. Statistical analysis

Data are presented as mean ± SEM. Statistical analyses were performed using Microsoft Excel (Microsoft Corporation, USA), Origin (OriginLab Corporation, USA) and Prism (Graphpad Software Inc., USA). Comparisons were made using one-way or two-way ANOVA with Bonferroni post-hoc comparison, paired *t*-test or one sample *t*-test as appropriate; $P < 0.05$ was taken as significant.

3. Results

3.1. KB-R7943 inhibits spontaneous action potentials and $[Ca^{2+}]_i$ transients

Fig. 1A shows a recording of the effect of rapid application of 5 μM KB-R7943 on spontaneous APs from a representative AVN cell. In the presence of KB-R7943, spontaneous AP amplitude progressively decreased as a result of a decrease in maximal diastolic potential (MDP) and overshoot potential, until APs disappeared, followed by the appearance of small oscillations of membrane potential. Spontaneous activity was restored on drug washout. KB-R7943 caused similar behaviour in 14 cells. All cells stopped generating APs within ~90 s of drug application, with a mean 'resting' potential in quiescent cells of −26.0 ± 2.1 mV. Of these, 6 cells became silent within 40 s of KB-R7943, whilst 8 cells became quiescent between 40 and 90 s. Table 1 shows mean AP parameters in control and after 15 and 40 s in the presence of KB-R7943, incorporating data from all cells studied ($n = 14$). Data were analysed at 15 s to determine the early effects of KB-R7943 and at 40 s as the time-point at which nearly half of the cells were quiescent, considering both APs and $[Ca^{2+}]_i$ transients. KB-R7943 decreased the slope of diastolic depolarization and AP rate, as well as MDP and maximum overshoot potential. However, for cells that did not stop within 40 s of drug application, there was only a modest decrease in spontaneous AP rate, from 3.75 ± 0.67 to 3.27 ± 0.29 beats/s (ns) at this time-point. Fig. 1B shows a representative recording of the effect of 5 μM KB-R7943 on spontaneous $[Ca^{2+}]_i$ transients, showing that they were slowed and then abolished by KB-R7943. This effect was reversible on washout of KB-R7943. In 6 out of 12 cells, the $[Ca^{2+}]_i$ transient stopped within 40 s. Table 2 shows mean data in control and after 15 and 40 s exposure to KB-R7943, incorporating data from all cells studied ($n = 12$). KB-R7943 decreased $[Ca^{2+}]_i$ transient rate, diastolic (baseline) Ca^{2+}, $[Ca^{2+}]_i$ transient peak and amplitude (Table 2). In cells that did not stop within 40 s, the spontaneous $[Ca^{2+}]_i$ transient rate decreased from 2.85 ± 0.30 to 1.17 ± 0.23 beats/s ($P < 0.01$) at 40 s.

Although KB-R7943 has been used as a selective inhibitor of NCX [8,15–17], it is not entirely selective [30]. Moreover, whilst many of the above effects of KB-R7943 are consistent with the hypothesis that NCX is involved in pacemaker activity (see Section 4), a reduction in AP upstroke velocity and overshoot potential are difficult to explain solely on the basis of an effect of KB-R7943 on NCX. Conse-

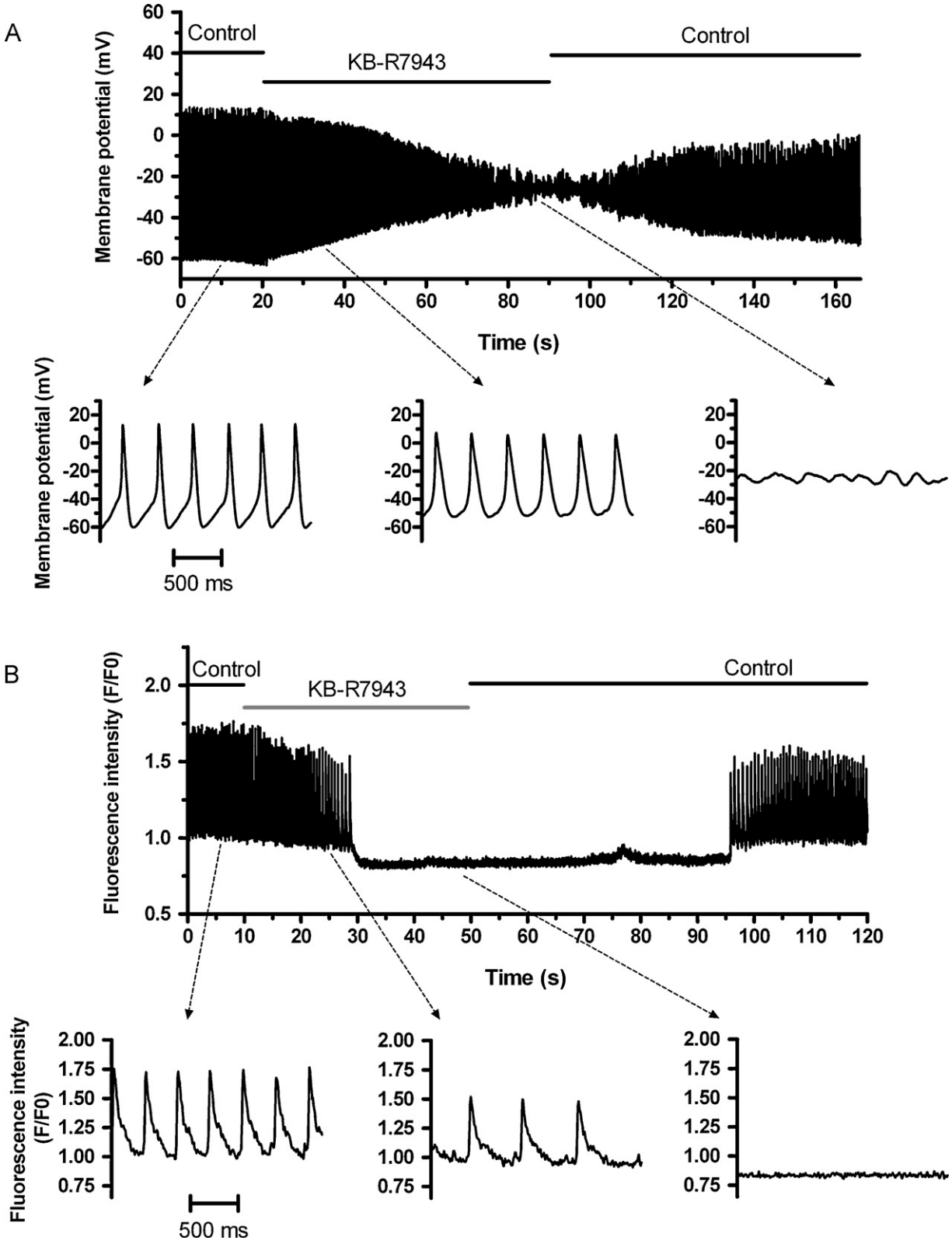

Fig. 1. Effects of KB-R7943 on spontaneous action potentials and $[Ca^{2+}]_i$ transients. (A) KB-R7943 inhibits spontaneous action potentials. The top trace shows a representative slow time-base recording of membrane potential from an AVN myocyte before, during and after exposure to 5 μM KB-R7943, as indicated by the horizontal bars above the trace. The lower traces show sections of the top panel from the periods indicated, in the absence (left) and presence (middle and right) of KB-R7943, displayed at a faster time-base. The time scale bar in the lower left panel applies to all three lower panels. (B) KB-R7943 inhibits spontaneous $[Ca^{2+}]_i$ transients. The top trace shows a slow time-base averaged fluorescence plot of confocal line-scan image from an AVN myocyte (different cell from A) before, during and after application of 5 μM KB-R7943, as indicated above the trace. The lower traces show sections of the top panel from the periods indicated, in the absence (left) and presence (middle and right) of KB-R7943, displayed at a faster time-base. The time scale bar in the lower left panel applies to all three lower panels.

Table 1
Effect of 5 μM KB-R7943 on spontaneous action potentials (APs) in rabbit atrioventricular node cells ($n = 14$).

Parameters	Control	At 15 s after KB-R7943 exposure	At 40 s after KB-R7943 exposure
Spontaneous AP rate (beats/s)	3.99 ± 0.47	3.64 ± 0.46	1.87 ± 0.48*
[% change, compared with control]		[−3.2 ± 13.9%]	[−40.4 ± 17.0%]
Slope of pacemaker diastolic depolarization (mV s^{-1})	113.9 ± 13.3	64.5 ± 8.2**	32.4 ± 8.8**
[% change]		[−34.2 ± 10.0%]	[−67.5 ± 9.8%]
Maximal upstroke velocity (V_{max}, V s^{-1})	5.76 ± 0.99	3.03 ± 0.81**	1.24 ± 0.48**
[% change]		[−50.0 ± 6.0%]	[−81.5 ± 5.2%]
Maximal repolarization velocity (V_{rep}, V s^{-1})	−1.53 ± 0.16	−0.92 ± 0.09**	−0.45 ± 0.12**
[% change]		[−37.1 ± 6.4%]	[−68.5 ± 8.1%]
AP duration at 50% repolarization (APD_{50}, ms)	63.24 ± 6.09	67.23 ± 6.83	50.29 ± 12.81
[% change]		[12.7 ± 13.2%]	[−19.2 ± 20.4%]
Maximal diastolic potential (MDP, mV)	−55.08 ± 1.85	−44.69 ± 2.21**	−35.40 ± 2.90**
[% change]		[−18.7 ± 3.3%]	[−35.8 ± 4.7%]
Overshoot (peak of AP, mV)	18.59 ± 2.05	4.18 ± 4.38**	−9.92 ± 5.11**
AP amplitude (mV)	73.68 ± 2.89	48.87 ± 5.90**	25.48 ± 6.95**
[% change]		[−34.2 ± 6.9%]	[−65.9 ± 8.8%]

When the data were analysed for this table, if the cell had stopped beating in the presence of KB-R7943, the values for maximal diastolic potential and peak of AP were taken as the 'resting' potential, and the values for AP rate and other parameters were taken as 0.
* $P < 0.05$ versus control.
** $P < 0.01$ versus control.

quently, to clarify the effects of KB-R7943 on AVN cell activity we investigated its effects on AVN I_{NCX} and $I_{Ca,L}$.

3.2. Inhibition by KB-R7943 of AVN I_{NCX}

I_{NCX} was elicited using voltage ramps from +60 to −80 mV with major interfering currents blocked (see Section 2 and [12]). Fig. 2Ai shows mean net current density–voltage relations under control conditions and in the presence of 5 μM KB-7943 or 5 mM Ni^{2+}. In control solution the voltage ramp elicited an outwardly rectifying current which was markedly reduced in amplitude in the presence of 5 μM KB-R7943 or 5 mM Ni^{2+} ($P < 0.001$). From these net current recordings, I_{NCX} was obtained as the Ni^{2+}-sensitive current (Fig. 2Aii, control – nickel). The KB-R7943-sensitive current (Fig. 2Aii, control – KB-R7943) was similar to the Ni^{2+}-sensitive current at potentials negative to the observed reversal potential (E_{rev}) over the voltage range studied, although the drug-sensitive current was slightly smaller than the Ni^{2+}-sensitive current at positive voltages (between +20 and +60 mV; $P < 0.05$, two-way ANOVA with Bonferroni post-hoc comparison). Examination of the residual KB-R7943 insensitive component of I_{NCX} ((control – nickel) – (control – KB-R7943) in Aii) showed no current at negative voltages (indicating that 5 μM KB-R7943 was as effective as Ni^{2+} at negative voltages), whilst at potentials positive to E_{rev} there was some residual I_{NCX} in the presence of KB-R7943.

Fig. 2B illustrates the time-course of effect of KB-R7943. Fig. 2Bi shows a representative plot of outward current (measured at +60 mV) against time, whilst Fig. 2Bii shows inward current (measured at −80 mV) from the same cell. Rapid application of either Ni^{2+} or KB-R7943 led to rapid changes of both inward and outward currents. However, although both agents caused almost complete inhibition of peak inward current, only Ni^{2+} completely inhibited peak outward current: some residual outward current remained at +60 mV in the presence of KB-R7943. These results show that 5 μM KB-R7943 was able to inhibit AVN I_{NCX} rapidly and completely at voltages relevant to the diastolic depolarization of AVN cells.

3.3. KB-R7943 inhibition of $I_{Ca,L}$

Fig. 3A shows representative traces of $I_{Ca,L}$ elicited in an AVN cell by depolarization from −40 mV to 0 mV (see Section 2), before, during and after application of 5 μM KB-R7943, which caused a reduction in $I_{Ca,L}$ that was reversible on washout. Mean data showing the time-course and extent of inhibition of $I_{Ca,L}$ are shown in Fig. 3B; KB-R7943 reduced $I_{Ca,L}$ at 0 mV from −18.57 ± 1.54 to −14.72 ± 1.28 pA/pF (a 20 ± 6% decrease; $P < 0.01$ versus control solution, $n = 12$) after 15 s exposure to KB-R7943 and to −12.68 ± 1.06 pA/pF (a 31 ± 6% decrease; $P < 0.01$ versus control solution, $n = 12$) after 40 s exposure to KB-R7943. After 90 s exposure to KB-R7943, $I_{Ca,L}$ was −11.94 ± 1.42 pA/pF (ns, compared to

Table 2
Effect of 5 μM KB-R7943 on spontaneous $[Ca^{2+}]_i$ transients in rabbit atrioventricular node cells ($n = 12$).

Parameters	Control	At 15 s after KB-R7943 exposure	At 40 s after KB-R7943 exposure
Spontaneous $[Ca^{2+}]_i$ transient rate (beats/s)	3.05 ± 0.24	1.35 ± 0.24**	0.58 ± 0.21**
[% change, compared with control]		[−53.0 ± 8.0%]	[−79.1 ± 7.4%]
Percentage increase of diastolic Ca^{2+} baseline compared with control (%)	–	−9.3 ± 3.2$$	−16.9 ± 2.8$$
$[Ca^{2+}]_i$ transient peak (F/F_0) (F: the peak fluorescence intensity; F_0: the control diastolic Ca^{2+} baseline)	1.64 ± 0.08	1.44 ± 0.12	1.16 ± 0.12**
[% change]		[−13.1 ± 3.5%]	[−29.2 ± 4.8%]
$[Ca^{2+}]_i$ transient amplitude between baseline and peak (F/F_0) (F: the difference of fluorescence intensity between baseline and peak; F_0: the control diastolic Ca^{2+} baseline)	0.64 ± 0.08	0.53 ± 0.11	0.33 ± 0.12**
[% change]		[−27.6 ± 10.4%]	[−60.6 ± 12.7%]

When the data were analysed for this table, if spontaneous $[Ca^{2+}]_i$ transients had stopped in the presence of KB-R7943, diastolic Ca^{2+} and $[Ca^{2+}]_i$ transient peak had the same values, and spontaneous $[Ca^{2+}]_i$ transient rate and $[Ca^{2+}]_i$ transient amplitude were taken as 0.
** $P < 0.01$ versus control.
$$ $P < 0.01$ compared with 0.

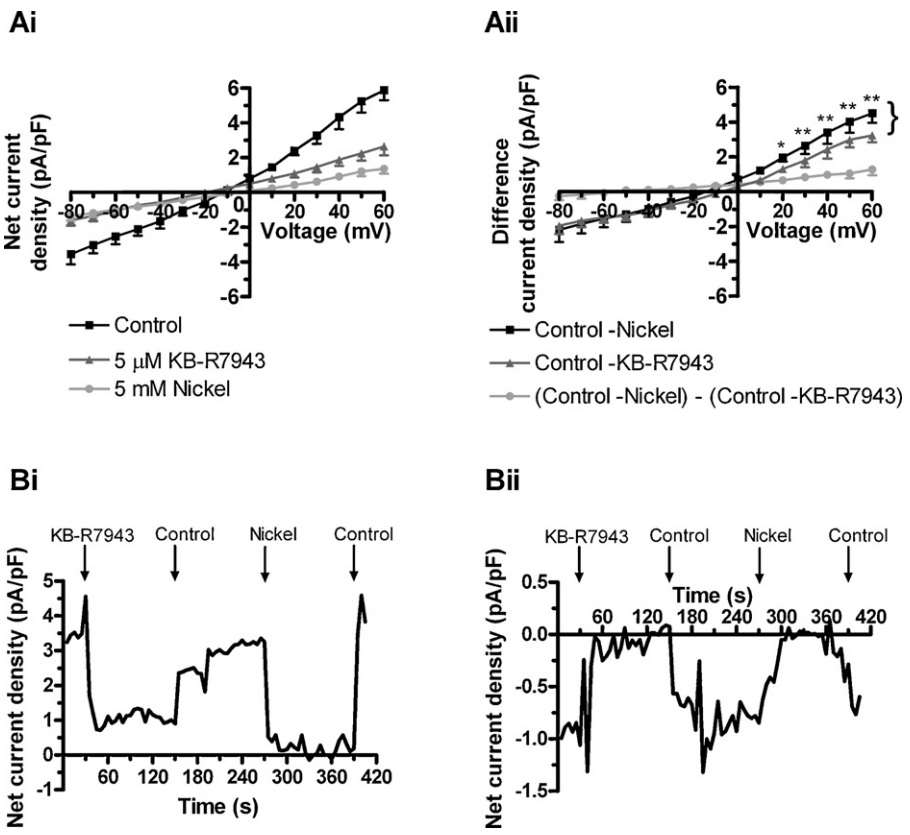

Fig. 2. KB-R7943 inhibits the nickel-sensitive I_{NCX} in rabbit AVN cells. (Ai) Mean net current densities recorded by a ramp protocol from +60 to −80 mV (duration = 250 ms, holding potential = −40 mV, frequency = 0.33 Hz) from AVN myocytes (n = 5) during superfusion with the control solution and exposure to 5 μM KB-R7943 or 5 mM nickel chloride. (Aii) Control – nickel represents the nickel-sensitive I_{NCX} density by subtracting the current density during exposure to nickel from that in control; control – KB-R7943 represents the KB-R7943-sensitive current; and (control – nickel) – (control – KB-R7943) represents the residual nickel-sensitive I_{NCX} after KB-R7943 inhibition. $^{*}P < 0.05$, $^{**}P < 0.01$: control – nickel versus control – KB-R7943. (Bi and Bii) Representative time-courses of the net current densities obtained at +60 mV (Bi) and −80 mV (Bii) from an AVN cell during superfusion with the control solution and exposure to 5 μM KB-R7943 and 5 mM nickel as indicated.

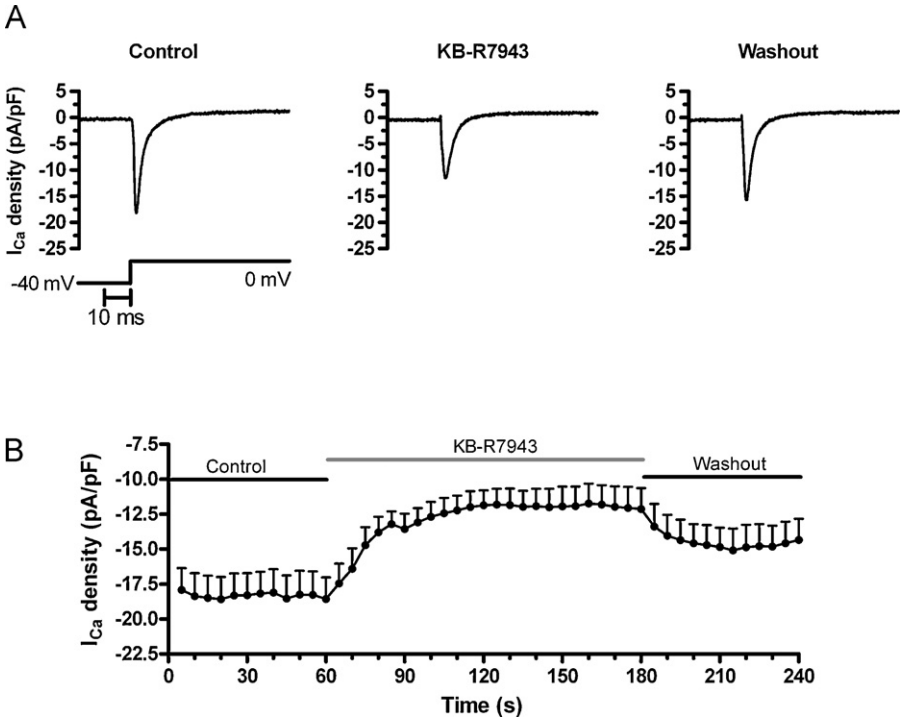

Fig. 3. KB-R7943 inhibits $I_{Ca,L}$ in rabbit AVN cells. (A) Representative $I_{Ca,L}$ traces from an AVN myocyte in the absence (control) and presence of 5 μM KB-R7943 and on washout, as indicated. The corresponding protocol used to elicit $I_{Ca,L}$ and the time scale bar are shown underneath. (B) The time-course of mean $I_{Ca,L}$ densities (at 0 mV, protocol shown as in A) from AVN myocytes (n = 12) in absence (control) and presence of 5 μM KB-R7943 (and following washout), as indicated.

40 s). These effects were rapidly but only partially reversed on washout (peak current recovered to −14.85 ± 1.39 pA/pF; 80 ± 7% of control). Thus, 5 μM KB-R7943 was partially able to inhibit $I_{Ca,L}$ over a time-course similar to that over which the compound affected spontaneous APs.

Given the observations in Figs. 2 and 3, additional experiments were performed using a lower concentration of 0.2 μM KB-R7943 in an attempt to inhibit NCX without affecting $I_{Ca,L}$. However, although spontaneous APs and $[Ca^{2+}]_i$ transient rates were reduced (by 41 ± 18% ($P < 0.05$, $n = 9$), and 70 ± 16% ($P < 0.01$, $n = 10$), respectively), both I_{NCX} and $I_{Ca,L}$ were still affected: Ni^{2+}-sensitive inward I_{NCX} at −80 mV was inhibited 84 ± 10% ($P < 0.01$, $n = 3$), whilst peak $I_{Ca,L}$ was decreased by 23 ± 5% ($P < 0.01$, $n = 7$).

To investigate the possible contribution of decreased $I_{Ca,L}$ to the effect of KB-R7943 on spontaneous activity, we empirically determined a concentration of the Ca^{2+} channel blocker nifedipine (0.2 μM) that produced approximately the same fractional decrease of $I_{Ca,L}$ as that observed in response to KB-R7943. This concentration of nifedipine significantly ($P < 0.01$; $n = 6$) decreased I_{Ca} from −17.72 ± 2.38 pA/pF to −12.46 ± 1.84 pA/pF (i.e. by 29.9 ± 4.1%) after 15 s, −13.09 ± 1.51 (by 25.2 ± 2.2%) after 30 s, and −12.77 ± 1.40 (by 26.7 ± 2.2%) after 60 s exposure. This concentration of nifedipine decreased spontaneous AP rate by 11.8 ± 4.6% ($P < 0.05$ versus control) after 15 s, by 12.1 ± 3.1% after 30 s ($P < 0.01$ versus control; not significantly different from effect at 15 s), and by 10.7 ± 4.4% after 60 s ($P < 0.05$ versus control; not significantly different from effect at 15 or 30 s). Interestingly, these percentage decreases in rate are similar to the 13% decrease observed in cells which did not stop beating in response to KB-R7943 (above). However, in contrast to the response to KB-R7943, 90 s exposure to nifedipine had little effect on maximum diastolic potential and did not cause cessation of spontaneous APs; nifedipine did, however, significantly ($P < 0.05$) decrease upstroke velocity, by 33.7 ± 4.2%, 44.4 ± 6.2%, and 44.6 ± 6.8% after 15, 30 and 60 s exposure, respectively, and significantly ($P < 0.01$) decreased action potential overshoot by 47.4 ± 8.5%, 46.4 ± 9.0%, and 50.3 ± 10.3% after 15, 30 and 60 s exposure, respectively.

3.4. Low extracellular sodium ($[Na^+]_e$) inhibits spontaneous action potentials

Application of low $[Na^+]_e$, has been shown previously to abolish spontaneous $[Ca^{2+}]_i$ transients from AVN cells at ambient temperature [13]. In light of this and the observed effects of KB-R7943 on $I_{Ca,L}$ (Fig. 3), $[Na^+]_e$ reduction (to 40 mM; see Section 2) was used to reduce forward mode NCX activity. In 9 out of 11 cells, reduction of $[Na^+]_e$ caused spontaneous APs to stop rapidly within ∼5 s. In the remaining 2 cells, although spontaneous APs did not stop with brief (∼10 s) exposure to low $[Na^+]_e$, the AP rate decreased by 27% ($P < 0.05$; versus control solution, $n = 2$), and then recovered following return to control solution. Sustained exposure to low $[Na^+]_e$ was not possible in these experiments as this led to cell contracture under our conditions.

3.5. SERCA blockade inhibits spontaneous activity

Thapsigargin and CPA were used to investigate the effect of depleting the SR by inhibiting SR Ca^{2+} uptake. Fig. 4A shows the effect of rapid application of 2.5 μM thapsigargin [31] on spontaneous APs. After exposure to thapsigargin, spontaneous AP rate initially increased and then decreased before stopping. Spontaneous APs stopped within 30 s in 3 out of 10 cells, and in all cells after ∼90 s. Spontaneous $[Ca^{2+}]_i$ transients showed a similar response: Fig. 4B shows a representative recording of the effect of thapsigargin on spontaneous $[Ca^{2+}]_i$ transients. On initial exposure to thapsigargin, diastolic Ca^{2+} and spontaneous rate increased; this was followed by a decrease in diastolic Ca^{2+} and a progressive decrease in rate and cessation of spontaneous $[Ca^{2+}]_i$ transients. Thapsigargin caused cessation of spontaneous $[Ca^{2+}]_i$ transients within 30 s in 5 out of 7 AVN cells, and after 60 s in all 7 cells. Table 3 shows mean data illustrating the time-course of the effect of thapsigargin on AP and $[Ca^{2+}]_i$ transient parameters (at 5, 15 and 30 s exposure to thapsigargin, incorporating measurements from all cells studied. By 60 s all cells were quiescent). The effects of thapsigargin were time-dependent (Table 3 and Fig. 4) and irreversible. Spontaneous AP frequency and slope of diastolic depolarization initially increased slightly (albeit ns) at 5 s, and then decreased following 15 and 30 s exposure to thapsigargin. Maximum diastolic potential and AP amplitude decreased progressively in the presence of thapsigargin. The $[Ca^{2+}]_i$ transient rate initially increased at 5 s and then decreased following 15 and 30 s exposure to thapsigargin; diastolic calcium initially increased slightly (albeit ns) and subsequently decreased during exposure to the compound.

CPA (30 μM) was also used to inhibit SERCA. Its effects on spontaneous activity were similar to those of thapsigargin. In brief, after 30 s exposure to CPA, spontaneous APs had ceased in 3 out of 9 cells, and $[Ca^{2+}]_i$ transients had ceased in 6 out of 10 cells; spontaneous action potentials and $[Ca^{2+}]_i$ transients had ceased in all cells after 90 s exposure to CPA. Incorporating data from all cells studied ($n = 9$ for APs, $n = 10$ for $[Ca^{2+}]_i$ transients), spontaneous AP frequency initially increased by 6.9 ± 3.0% after 5 s ($P < 0.05$ versus control) and then decreased by 58.4 ± 11.8% ($P < 0.01$ versus control) after 30 s exposure to CPA. Similarly, $[Ca^{2+}]_i$ transient frequency initially increased, by 64.1 ± 17.6% after 5 s ($P < 0.01$ versus control) and then decreased by 66.9 ± 16.1% ($P < 0.05$ versus control) after 30 s exposure to CPA.

4. Discussion

4.1. Actions of the NCX inhibitor KB-R7943

KB-R7943 has been used widely in experiments on intact hearts, isolated cardiac tissues and cells (e.g. [8,15–18]). When KB-R7943 was first tested on guinea-pig ventricular I_{NCX}, it was reported to exhibit preferential inhibition of outward I_{NCX} (i.e. reverse mode NCX) [32], however it was found subsequently to inhibit both modes of NCX function under bi-directional I_{NCX} recording conditions [15,33]. This compound has been used in experiments that implicated NCX in canine SAN activity [34] and, at the same concentration as used here, has also been reported to inhibit spontaneous activity of guinea-pig isolated SAN cells [8]. However, to our knowledge the present study is the first in which this agent has been used in experiments on an AVN preparation. Under our conditions, 5 μM KB-R7943 produced bi-directional block of AVN I_{NCX}, though with an apparent preference for inward I_{NCX} (i.e. forward mode NCX). 5 mM Ni^{2+} is an effective inhibitor of I_{NCX} when used under NCX-selective conditions [35,36]. Thus, the similarity of inward KB-R7943-sensitive current and Ni^{2+}-sensitive inward current under I_{NCX}-selective conditions suggests a maximal or near maximal inhibition of forward mode I_{NCX} at this concentration of KB-R7943. NCX can be anticipated to be operating in the forward mode (inward I_{NCX}) over the diastolic potential range of AVN cells. Thus, the marked effect of KB-R7943 on AVN cell spontaneous rate (for both APs and $[Ca^{2+}]_i$ transients) is consistent with a significant role for NCX in AVN pacemaking. This notion is supported by the inhibitory effect of rapid application of a low $[Na^+]_e$ solution at physiological (this study) and ambient (reported previously [13]) temperatures.

However, KB-R7943 is not entirely selective for NCX: Kimura and colleagues found that the compound inhibited I_{Na}, $I_{Ca,L}$ and the inward rectifier K^+ current I_{K1} with IC_{50} values of 14, 8 and 7 μM respectively [32]. Rabbit AVN cells lack I_{K1} [21,26] and Na chan-

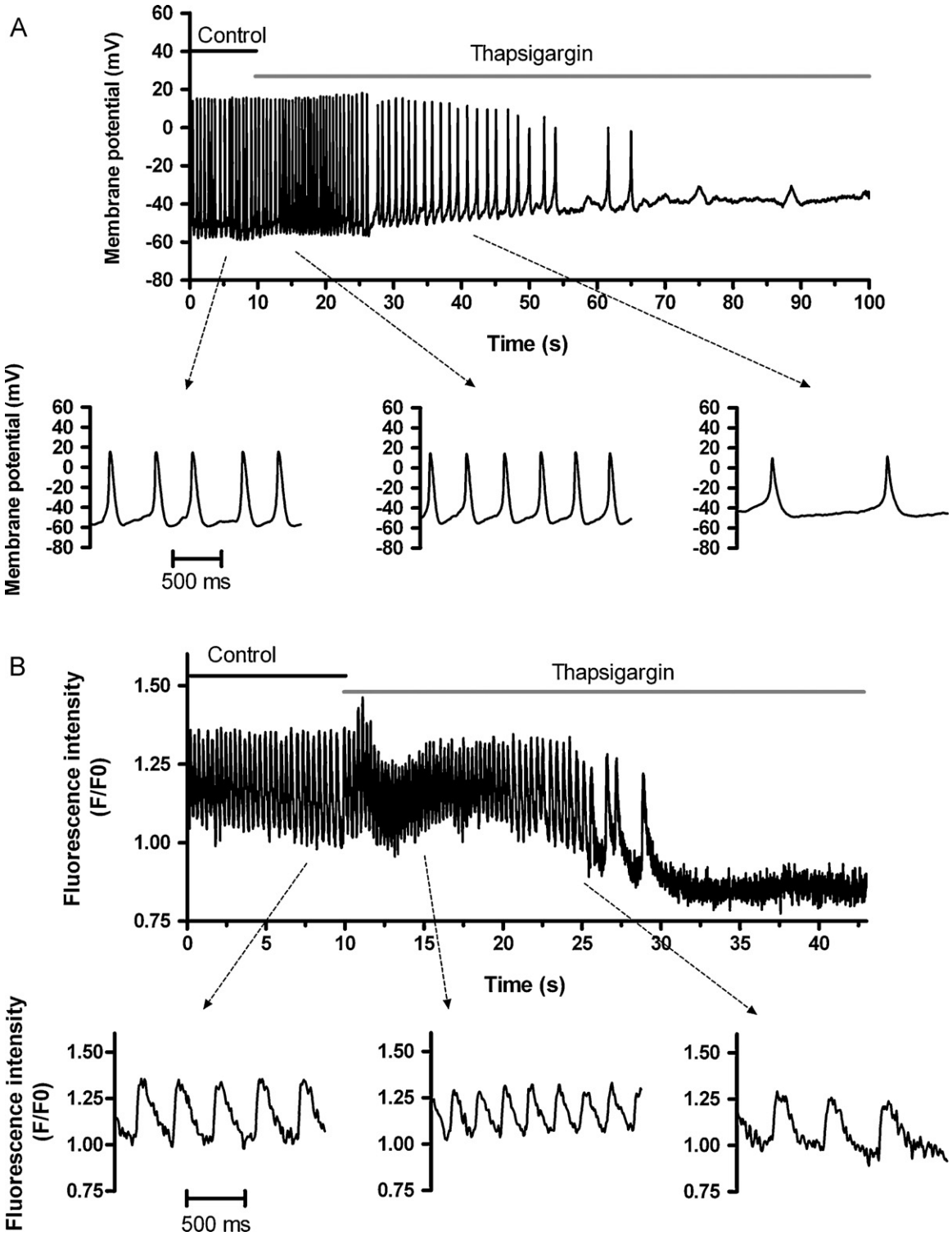

Fig. 4. Effects of thapsigargin on spontaneous action potentials and $[Ca^{2+}]_i$ transients. (A) Thapsigargin inhibits spontaneous action potentials. The top trace shows a slow time-base recording of membrane potential from a representative AVN myocyte before, during and after application of 2.5 μM thapsigargin, as indicated above the trace. The lower traces show sections of the top panel from the periods indicated, in the absence (left) and presence (middle and right) of thapsigargin, displayed at a faster time-base. The time scale bar in the lower left trace applies to all three lower traces. In the first few seconds after thapsigargin exposure, initially the spontaneous AP rate increased and then decreased, with cessation of activity at ~60 s after thapsigargin exposure. (B) Thapsigargin inhibits spontaneous $[Ca^{2+}]_i$ transients. The top trace shows a slow time-base averaged fluorescence plot of a confocal line-scan image from a representative AVN myocyte (different cell from A) before, during and after application of 2.5 μM thapsigargin as indicated above the trace. The lower panels show sections of the top trace from the periods indicated, in the absence (left) and presence (middle and right) of thapsigargin, displayed at a faster time-base. The time scale bar in the lower left trace applies to all three lower traces. In the first few seconds after thapsigargin exposure, initially the $[Ca^{2+}]_i$ transient rate increased, and the diastolic calcium baseline was elevated; the spontaneous $[Ca^{2+}]_i$ transient rate then decreased and stopped at ~20 s following thapsigargin exposure.

Table 3
Effect of 2.5 μM thapsigargin on spontaneous $[Ca^{2+}]_i$ transients and action potentials (APs) in rabbit atrioventricular node cells.

Parameters	Control	At 5 s after thapsigargin exposure	At 15 sec after thapsigargin exposure	At 30 s after thapsigargin exposure
Spontaneous AP ($n = 10$)				
Rate (beats/s)	3.22 ± 0.25	3.40 ± 0.33	2.44 ± 0.36*	1.48 ± 0.44**
[% change, compared with control]		[5.6 ± 4.3%]	[−25.1 ± 6.9%]	[−57.8 ± 10.9%]
Slope of pacemaker diastolic depolarization (mV s^{-1})	97.7 ± 18.9	102.0 ± 17.6	68.1 ± 18.5*	33.6 ± 10.3**
[% change]		[12.6 ± 12.1%]	[−31.9 ± 7.4%]	[−65.1 ± 11.7%]
Maximal diastolic potential (MDP, mV)	−52.74 ± 3.09	−50.55 ± 3.02	−50.68 ± 2.71	−46.31 ± 2.47*
[% change]		[−4.1 ± 1.4%]	[−3.6 ± 1.6%]	[−11.5 ± 3.5%]
AP amplitude (mV)	63.96 ± 3.99	59.65 ± 3.75	59.68 ± 4.46	43.20 ± 9.82*
[% change]		[−6.5 ± 1.9%]	[−7.2 ± 3.7%]	[−35.0 ± 14.4%]
Spontaneous $[Ca^{2+}]_i$ transient ($n = 7$)				
Rate (beats/s)	3.27 ± 0.41	4.36 ± 0.36*	1.95 ± 0.56*	0.35 ± 0.34**
[% change, compared with control]		[38.7 ± 13.1%]	[−43.9 ± 13.1%]	[−87.5 ± 12.5%]
Percentage increase of diastolic Ca^{2+} baseline compared with control (%)	–	4.52 ± 2.49%	−7.05 ± 4.89	−27.47 ± 7.21$^{\$\$}$

When the data were analysed for this table, if spontaneous activity had stopped in the presence of thapsigargin, the values for maximal diastolic potential were taken as the 'resting' potential, and the values for AP rate and other AP parameters were taken as 0; and spontaneous $[Ca^{2+}]_i$ transient rate was taken as 0.
* $P < 0.05$, versus control.
** $P < 0.01$ versus control.
$^{\$\$}$ $P < 0.01$ compared with 0.

nels are sparse or absent from the compact node [37]; moreover, the maximal upstroke velocity of AVN control APs in our KB-R7943 experiments (<6 V s^{-1}) is inconsistent with a major role for I_{Na} in driving the AP upstroke in the cells studied here. Thus, effects of KB-R7943 on I_{Na} or I_{K1} are unlikely to have contributed significantly to the effects of this agent observed in the present study. On the other hand, $I_{Ca,L}$ plays a major role in AP genesis [38,39]. Under our conditions 5 μM KB-R7943 inhibited $I_{Ca,L}$ by ∼31%, which is compatible with earlier ventricular cell data [30,32,33]. This secondary action of KB-R7943 is likely to contribute significantly to changes to AP upstroke velocity and overshoot seen here, whilst progressive depolarization in MDP may also have contributed via facilitating I_{CaL} inactivation. When the role of $I_{Ca,L}$ was tested by investigating the effect of a nifedipine concentration that produced a similar decrease of $I_{Ca,L}$ to KB-R7943, this compound produced a marked effect on AP upstroke velocity and overshoot, consistent with the established role of $I_{Ca,L}$ in AVN APs [38,39]. However, in no cell studied did nifedipine induce quiescence (although spontaneous AP rate decreased by ∼12%). Thus, any secondary effect of KB-R7943 on $I_{Ca,L}$ is likely only to have had a comparatively minor effect on spontaneous AP rate, and the observed cessation of spontaneous activity in KB-R7943-treated cells is unlikely to be attributable to an effect on $I_{Ca,L}$. The 'resting' potential at which cells became quiescent in KB-R7943 (−26 mV) is more positive than the known zero current potential of AVN cells (−40 mV [21,26]). This may suggest an additional action of KB-R7943, potentially on an outward resting conductance. Although this avenue was not pursued in the present study, an inhibitory effect on delayed rectifier K^+ current has been reported [30] and the rapid delayed rectifier (I_{Kr}) is active during AVN AP repolarization and the diastolic depolarization [14,40,41].

4.2. Influence of SERCA inhibition on AVN spontaneous activity

Recent studies have shown that inhibition of ryanodine receptors (RyRs) in AVN cells has a marked inhibitory effect on spontaneous AP and calcium transient rate [13,14]. If SR Ca^{2+} release is involved in AVN cell pacemaking, then inhibition of SR Ca^{2+} reuptake by inhibition of SERCA would also be predicted to reduce spontaneous rate. Indeed, SERCA inhibition has been observed to slow the spontaneous rate of guinea-pig [3,8], canine [42] and rabbit [43] SAN preparations. The immediate effect of SERCA inhibition by both thapsigargin and CPA in the present study was an initial increase in diastolic $[Ca^{2+}]_i$ and in spontaneous AP and $[Ca^{2+}]_i$ transient rate. This is consistent with a scheme in which transiently raised $[Ca^{2+}]_i$, due to reduced SR reuptake of Ca^{2+}, leads to greater activation of a sarcolemmal electrogenic process (most likely involving the NCX, as discussed above). The subsequent decline in spontaneous AP/$[Ca^{2+}]_i$ transient rate would be anticipated to follow this transient increase, once the SR were depleted of Ca^{2+} and this had been removed from the cytosol. In time, the loss of SR Ca^{2+} would in turn remove the influence of cyclic SR Ca^{2+} release on sarcolemmal electrogenicity. CPA was found to produce qualitatively similar results to thapsigargin; thus data with both agents implicate SR Ca^{2+} cycling in spontaneous activity.

In the SAN, a calcium "clock" has been proposed along with the traditional voltage clock (i.e. membrane currents generated by voltage-dependent ion channels) to bring about spontaneous activity [44,45]. It has been proposed that after a calcium transient of the SAN cell, as SR calcium content increases and ryanodine receptors (RyRs) recover from inactivation, high $[Ca^{2+}]$ in the SR lumen activates RyRs, causing a localized subsarcolemmal calcium release (i.e. a calcium spark) [46]. This causes a local increase of cytoplasmic $[Ca^{2+}]$, stimulating inward I_{NCX}. This brief inward current causes a small diastolic depolarization, with summation of such individual events bringing the membrane potential to threshold for an action potential. This rhythmic spontaneous SR Ca^{2+} release/spark shows inherent rhythmicity, giving rise to the term "calcium clock" [44,46]. In our previous study of AVN cells at ambient temperature calcium sparks occurred relatively infrequently [13] and in our present experiments calcium sparks were not detected in spontaneously beating AVN cells. It seems unlikely, therefore, that the calcium clock mechanism identified for the rabbit SAN [46] underpins the role of SR Ca^{2+} release in AVN cell pacemaking; our data are more consistent with a scheme in which Ca^{2+} transients initiated by the AP upstroke in turn activate sarcolemmal NCX to extrude Ca^{2+} generating an inward current that persists into diastole.

4.3. Strengths, limitations and conclusions

In comparison to the SAN [3,4,6–10,42–46], comparatively few data exist regarding Ca^{2+} handling by AVN cells [13,14]. The present results not only add new information about Ca^{2+} handling, but also further implicate SR Ca^{2+} cycling in electrogenicity of spontaneously active AVN cells. Caveats in the use of KB-R7943 are highlighted earlier in the 'Discussion'. The use of this compound is nevertheless warranted because it is arguably the most effective commercially available NCX inhibitor and because it has been used in prior cardiac studies [8,15–18,32–34]. The AVN is known to be a heterogeneous structure [1,21,47] and cells were isolated from the entire AVN region, so that it is not possible to attribute

with certainty AVN regional sub-types to individual cells studied. However, this uncertainty is shared with numerous previous AVN studies (e.g. [13,21,26]), and the relatively slow AP upstroke velocities observed here are most compatible with 'N-like' or 'NH-like' APs [47]. Although concurrent Ca^{2+} transient and AP recordings would permit changes to both events to be viewed in parallel, we found that a combination of Fluo-4 dye loading and whole-cell recording rapidly led to quiescence in nearly all cells studied in this way. Thus, in order to minimize cell dialysis and buffering of Ca^{2+} transients, Ca^{2+} transients and APs were therefore recorded in separate experiments. Nevertheless, the limited data that we have obtained recording both parameters simultaneously (not shown) showed no cyclic changes of $[Ca^{2+}]_i$ in the absence of APs; this is consistent with a scheme in which the AP upstroke initiates the SR Ca^{2+} release process which itself ultimately then influences diastolic depolarization. Our thapsigargin and CPA data demonstrate that inhibition of SERCA prevents effective Ca^{2+} cycling and thereby influences spontaneous activity. Inhibition of spontaneous activity by two KB-R7943 concentrations differing >20 fold, together with the inhibitory effect of low $[Na]_e$ strongly implicates the NCX as a major electrogenic transport process that couples SR Ca^{2+} release to spontaneous AP genesis. Further work is required to determine whether NCX is the only such process or whether, as has been suggested for the SAN, other mechanisms such as $[Ca^{2+}]_i$ sensitive cation channels [48] may also be involved.

Acknowledgments

This work was supported by the British Heart Foundation (PG 08/036/24905). We thank Drs Palash Barman and Stephanie Choisy for assistance with cell isolation and Mrs Lesley Arberry for technical assistance.

References

[1] F.L. Meijler, M.J. Janse, Morphology and electrophysiology of the mammalian atrioventricular node, Physiol. Rev. 68 (1988) 608–647.
[2] S. Tawara, Das Reizleitungssystem des Saugetierherzens, Fischer, Jena, Germany, 1906.
[3] L. Rigg, D.A. Terrar, Possible role of calcium release from the sarcoplasmic reticulum in pacemaking in guinea-pig sino-atrial node, Exp. Physiol. 81 (1996) 877–880.
[4] T. Hata, T. Noda, M. Nishimura, Y. Watanabe, The role of Ca^{2+} release from sarcoplasmic reticulum in the regulation of sinoatrial node automaticity, Heart Vessels 11 (1996) 234–241.
[5] J. Li, J. Qu, R.D. Nathan, Ionic basis of ryanodine's negative chronotropic effect on pacemaker cells isolated from the sinoatrial node, Am. J. Physiol. 273 (1997) H2481–H2489.
[6] K.Y. Bogdanov, T.M. Vinogradova, E.G. Lakatta, Sinoatrial nodal cell ryanodine receptor and Na^+–Ca^{2+} exchanger: molecular partners in pacemaker regulation, Circ. Res. 88 (2001) 1254–1258.
[7] V.A. Maltsev, T.M. Vinogradova, K.Y. Bogdanov, E.G. Lakatta, M.D. Stern, Diastolic calcium release controls the beating rate of rabbit sinoatrial node cells: numerical modeling of the coupling process, Biophys. J. 86 (2004) 2596–2605.
[8] L. Sanders, S. Rakovic, M. Lowe, P.A. Mattick, D.A. Terrar, Fundamental importance of Na^+–Ca^{2+} exchange for the pacemaking mechanism in guinea-pig sino-atrial node, J. Physiol. 571 (2006) 639–649.
[9] E.G. Lakatta, T.M. Vinogradova, K.Y. Bogdanov, Beta-adrenergic stimulation modulation of heart rate via synchronization of ryanodine receptor Ca^{2+} release, J. Card. Surg. 17 (2002) 451–461.
[10] T.M. Vinogradova, K.Y. Bogdanov, E.G. Lakatta, beta-Adrenergic stimulation modulates ryanodine receptor Ca^{2+} release during diastolic depolarization to accelerate pacemaker activity in rabbit sinoatrial nodal cells, Circ. Res. 90 (2002) 73–79.
[11] J.C. Hancox, A.J. Levi, P. Brooksby, Intracellular calcium transients recorded with Fura-2 in spontaneously active myocytes isolated from the atrioventricular node of the rabbit heart, Proc. Biol. Sci. 255 (1994) 99–105.
[12] M.K. Convery, J.C. Hancox, Na^+–Ca^{2+} exchange current from rabbit isolated atrioventricular nodal and ventricular myocytes compared using action potential and ramp waveforms, Acta Physiol. Scand. 168 (2000) 393–401.
[13] J.M. Ridley, H. Cheng, O.J. Harrison, S.K. Jones, G.L. Smith, J.C. Hancox, C.H. Orchard, Spontaneous frequency of rabbit atrioventricular node myocytes depends on SR function, Cell Calcium 44 (2008) 580–591.
[14] M.R. Nikmaram, J. Liu, M. Abdelrahman, H. Dobrzynski, M.R. Boyett, M. Lei, Characterization of the effects of ryanodine, TTX, E-4031 and 4-AP on the sinoatrial and atrioventricular nodes, Prog. Biophys. Mol. Biol. 96 (2008) 452–464.
[15] J. Kimura, T. Watano, M. Kawahara, E. Sakai, J. Yatabe, Direction-independent block of bi-directional Na^+/Ca^{2+} exchange current by KB-R7943 in guinea-pig cardiac myocytes, Br. J. Pharmacol. 128 (1999) 969–974.
[16] C.I. Spencer, J.S. Sham, Effects of Na^+/Ca^{2+} exchange induced by SR Ca^{2+} release on action potentials and after depolarizations in guinea pig ventricular myocytes, Am. J. Physiol. Heart Circ. Physiol. 285 (2003) H2552–H2562.
[17] M.S. Amran, N. Homma, K. Hashimoto, Pharmacology of KB-R7943: a Na^+–Ca^{2+} exchange inhibitor, Cardiovasc. Drug Rev. 21 (2003) 255–276.
[18] S.A. Doggrell, J.C. Hancox, Is timing everything? Therapeutic potential of modulators of cardiac Na^+ transporters, Expert Opin. Investig. Drugs 12 (2003) 1123–1142.
[19] A. Wrzosek, H. Schneider, S. Grueninger, M. Chiesi, Effect of thapsigargin on cardiac muscle cells, Cell Calcium 13 (1992) 281–292.
[20] N.J. Yard, M. Chiesi, H.A. Ball, Effect of cyclopiazonic acid, an inhibitor of sarcoplasmic reticulum Ca^{2+}-ATPase, on the frequency-dependence of the contraction-relaxation cycle of the guinea-pig isolated atrium, Br. J. Pharmacol. 113 (1994) 1001–1007.
[21] J.C. Hancox, A.J. Levi, C.O. Lee, P. Heap, A method for isolating rabbit atrioventricular node myocytes which retain normal morphology and function, Am. J. Physiol. 265 (1993) H755–H766.
[22] R.H. Anderson, M.J. Janse, F.J. van Capelle, J. Billette, A.E. Becker, D. Durrer, A combined morphological and electrophysiological study of the atrioventricular node of the rabbit heart, Circ. Res. 35 (1974) 909–922.
[23] G. Isenberg, U. Klockner, Calcium tolerant ventricular myocytes prepared by preincubation in a "KB medium", Pflugers Arch. 395 (1982) 6–18.
[24] J. Hancox, A. Levi, The hyperpolarisation-activated current, I_f, is not required for pacemaking in single cells from the rabbit atrioventricular node, Pflugers Arch. 427 (1994) 121–128.
[25] F.C. Howarth, A.J. Levi, J.C. Hancox, Characteristics of the delayed rectifier K current compared in myocytes isolated from the atrioventricular node and ventricle of the rabbit heart, Pflugers Arch. 431 (1996) 713–722.
[26] H. Cheng, G.L. Smith, C.H. Orchard, J.C. Hancox, Acidosis inhibits spontaneous activity and membrane currents in myocytes isolated from the rabbit atrioventricular node, J. Mol. Cell. Cardiol. 46 (2009) 75–85.
[27] J.C. Hancox, J.S. Mitcheson, Inhibition of L-type calcium current by propafenone in single myocytes isolated from the rabbit atrioventricular node, Br. J. Pharmacol. 121 (1997) 7–14.
[28] A.J. Levi, J.C. Hancox, F.C. Howarth, J. Croker, J. Vinnicombe, A method for making rapid changes of superfusate whilst maintaining temperature at 37 °C, Pflugers Arch. 432 (1996) 930–937.
[29] F. Brette, S. Despa, D.M. Bers, C.H. Orchard, Spatiotemporal characteristics of SR Ca^{2+} uptake and release in detubulated rat ventricular myocytes, J. Mol. Cell. Cardiol. 39 (2005) 804–812.
[30] H. Tanaka, K. Nishimaru, T. Aikawa, W. Hirayama, Y. Tanaka, K. Shigenobu, Effect of SEA0400, a novel inhibitor of sodium–calcium exchanger, on myocardial ionic currents, Br. J. Pharmacol. 135 (2002) 1096–1100.
[31] M. Hussain, C.H. Orchard, Sarcoplasmic reticulum Ca^{2+} content, L-type Ca^{2+} current and the Ca^{2+} transient in rat myocytes during beta-adrenergic stimulation, J. Physiol. 505 (Pt 2) (1997) 385–402.
[32] T. Watano, J. Kimura, T. Morita, H. Nakanishi, A novel antagonist, No. 7943, of the Na^+/Ca^{2+} exchange current in guinea-pig cardiac ventricular cells, Br. J. Pharmacol. 119 (1996) 555–563.
[33] P. Birinyi, K. Acsai, T. Banyasz, A. Toth, B. Horvath, L. Virag, N. Szentandrassy, J. Magyar, A. Varro, F. Fulop, P.P. Nanasi, Effects of SEA0400 and KB-R7943 on Na^+/Ca^{2+} exchange current and L-type Ca^{2+} current in canine ventricular cardiomyocytes, Naunyn Schmiedebergs Arch. Pharmacol. 372 (2005) 63–70.
[34] F. Kurogouchi, Y. Furukawa, D. Zhao, M. Hirose, K. Nakajima, M. Tsuboi, S. Chiba, A Na^+/Ca^{2+} exchanger inhibitor, KB-R7943, caused negative inotropic responses and negative followed by positive chronotropic responses in isolated, blood-perfused dog heart preparations, Jpn. J. Pharmacol. 82 (2000) 155–163.
[35] J. Kimura, S. Miyamae, A. Noma, Identification of sodium–calcium exchange current in single ventricular cells of guinea-pig, J. Physiol. 384 (1987) 199–222.
[36] A.K. Hinde, L. Perchenet, I.A. Hobai, A.J. Levi, J.C. Hancox, Inhibition of Na/Ca exchange by external Ni in guinea-pig ventricular myocytes at 37 °C, dialysed internally with cAMP-free and cAMP-containing solutions, Cell Calcium 25 (1999) 321–331.
[37] K. Petrecca, F. Amellal, D.W. Laird, S.A. Cohen, A. Shrier, Sodium channel distribution within the rabbit atrioventricular node as analysed by confocal microscopy, J. Physiol. 501 (Pt 2) (1997) 263–274.
[38] J.C. Hancox, A.J. Levi, L-type calcium current in rod- and spindle-shaped myocytes isolated from rabbit atrioventricular node, Am. J. Physiol. 267 (1994) H1670–H1680.
[39] S. Inada, J.C. Hancox, H. Zhang, M.R. Boyett, One-dimensional mathematical model of the atrioventricular node including atrio-nodal, nodal, and nodal-His cells, Biophys. J. 97 (2009) 2117–2127.
[40] N. Sato, H. Tanaka, Y. Habuchi, W.R. Giles, Electrophysiological effects of ibutilide on the delayed rectifier K^+ current in rabbit sinoatrial and atrioventricular node cells, Eur. J. Pharmacol. 404 (2000) 281–288.
[41] J.S. Mitcheson, J.C. Hancox, An investigation of the role played by the E-4031-sensitive (rapid delayed rectifier) potassium current in isolated rabbit atrioventricular nodal and ventricular myocytes, Pflugers Arch. 438 (1999) 843–850.

[42] B. Joung, L. Tang, M. Maruyama, S. Han, Z. Chen, M. Stucky, L.R. Jones, M.C. Fishbein, J.N. Weiss, P.S. Chen, S.F. Lin, Intracellular calcium dynamics and acceleration of sinus rhythm by beta-adrenergic stimulation, Circulation 119 (2009) 788–796.
[43] T.M. Vinogradova, D. Brochet, S. Sirenko, Y. Li, H. Spurgeon, E.G. Lakatta, Sarcoplasmic reticulum Ca^{2+} pumping kinetics regulates timing of local Ca^{2+} releases and spontaneous beating rate of rabbit sinoatrial node pacemaker cells, Circ. Res. 107 (2010) 767–775.
[44] B. Joung, M. Ogawa, S.F. Lin, P.S. Chen, The calcium and voltage clocks in sinoatrial node automaticity, Korean Circ. J. 39 (2009) 217–222.
[45] D.A. Eisner, E. Cerbai, Beating to time: calcium clocks, voltage clocks, and cardiac pacemaker activity, Am. J. Physiol. Heart Circ. Physiol. 296 (2009) H561–H562.
[46] T.M. Vinogradova, Y.Y. Zhou, V. Maltsev, A. Lyashkov, M. Stern, E.G. Lakatta, Rhythmic ryanodine receptor Ca^{2+} releases during diastolic depolarization of sinoatrial pacemaker cells do not require membrane depolarization, Circ. Res. 94 (2004) 802–809.
[47] A.A. Munk, R.A. Adjemian, J. Zhao, A. Ogbaghebriel, A. Shrier, Electrophysiological properties of morphologically distinct cells isolated from the rabbit atrioventricular node, J. Physiol. 493 (Pt 3) (1996) 801–818.
[48] Y.K. Ju, Y. Chu, H. Chaulet, D. Lai, O.L. Gervasio, R.M. Graham, M.B. Cannell, D.G. Allen, Store-operated Ca^{2+} influx and expression of TRPC genes in mouse sinoatrial node, Circ. Res. 100 (2007) 1605–1614.